

# Experiments on Unstiffened Thin Web Girders

*Deflections and deformations to failure are plotted to reveal behavior under load*

BY C. CHERN AND V. KUNAPONGSIRI

**ABSTRACT.** Two welded thin web plate girders without intermediate transverse stiffeners were tested under uniformly distributed loads. The girders were 24 inches deep and 11 feet long with the web depth to web thickness ratio of 192 and 384, respectively. The dimensions of girder specimens; the test set-up, the testing procedure and the observation of the test results are described and discussed.

The primary objective of this experiment was to investigate the behavior of the web plate of unstiffened thin web girders under uniformly distributed loads over the entire span. The results obtained herein supplied the information for developing an analytical approach for determining the static ultimate strength of the girders.

## Introduction

The essential difference between a welded plate girder and a rolled beam is the slenderness of the web. Because of this difference, the methods commonly used in the design of beams are not applicable to plate girder design.

During the past decade there has been a remarkable increase in the use of welded thin web plate girders in conjunction with the composite deck for roof and floor construction. One essential point is, regardless of the thin web, there is considerable fabrication cost due to the use of intermediate transverse stiffeners which have to be manually installed and welded in position. The advantages for developing unstiffened girders (i.e., a girder without intermediate transverse stiffeners) are: (a)

light weight, (b) simplicity in the sense of fabrication, and (c) use of automatic welding machines to reduce the fabrication costs.

However, present design specifications do not provide guide lines for the design of unstiffened thin web girders. The research project was started in 1971 in the Department of Civil Engineering, North Dakota State University with the primary objective of investigating the behavior of the web plate of unstiffened plate girders subjected to uniformly distributed load over the entire span. The observation of this experimentation provided information for developing an analytical approach for determining the static ultimate strength of the girders.

Presented herein is the experimental phase of the research. Two girders with web depth of 24 in. and span length of 10 ft were tested. The dimensions and material properties of the girder components, the test set-up, the testing procedure and the observations are described and discussed. The behavior of the web plate under increment loading is presented in the form of contour maps which were plotted with the aid of a computer.

## Testing Program

### Introduction

The primary objective of the testing program was to investigate the web behavior of the unstiffened thin web plate girders under uniformly distributed loading conditions. The testing program consisted of the static ultimate strength tests of two unstiffened girders. The girders were 11 ft long and 24 in. deep with a pair

---

### Nomenclature

- a = span length or the distance from center to center of the bearing stiffeners, inches  
b = web depth or the distance between the inner surface of the flanges, inches  
t = web thickness, inches  
v = vertical deflection of the flanges, inches  
w = lateral deflection of the web plate, inches  
x,y,z = cartesian coordinate axes  
P = load applied on each hydraulic jack, kips  
 $P_u$  = experimentally obtained ultimate load per jack, kips  
 $\alpha$  = (a/b) aspect ratio or the ratio of the span length to the web depth  
 $\beta$  = (b/t) web slenderness ratio or the ratio of the web depth to web thickness  
 $\sigma_y$  = yield stress, ksi  
 $\sigma_u$  = ultimate tensile stress, ksi
- 

---

C. CHERN is Assistant Professor of Civil Engineering, North Dakota State University, Fargo, N.D. and V. KUNAPONGSIRI is Project Engineer, Dept. of Highways, Bangkok, Thailand (formerly graduate assistant, Dept. of Civil Engineering North Dakota State University).

Paper to be presented at ASCE National Structural Engineering Meeting, San Francisco, April 9-13, 1973.

**Table 1 — Dimensions and Test Results**

Girder No.	Flange		Web		Span length, in.	Aspect ratio, ( $\alpha$ )	Slender-ness ratio, ( $\beta$ )	Failure load, <sup>(a)</sup> kips
	Width, in.	Thick-ness, in.	Depth, in.	Thick-ness, in.				
A	5.0	0.312	24.0	0.126	120.0	5.0	192	11.85
B	5.0	0.312	24.0	0.062	120.0	5.0	384	3.00

(a) Test failure load per jack

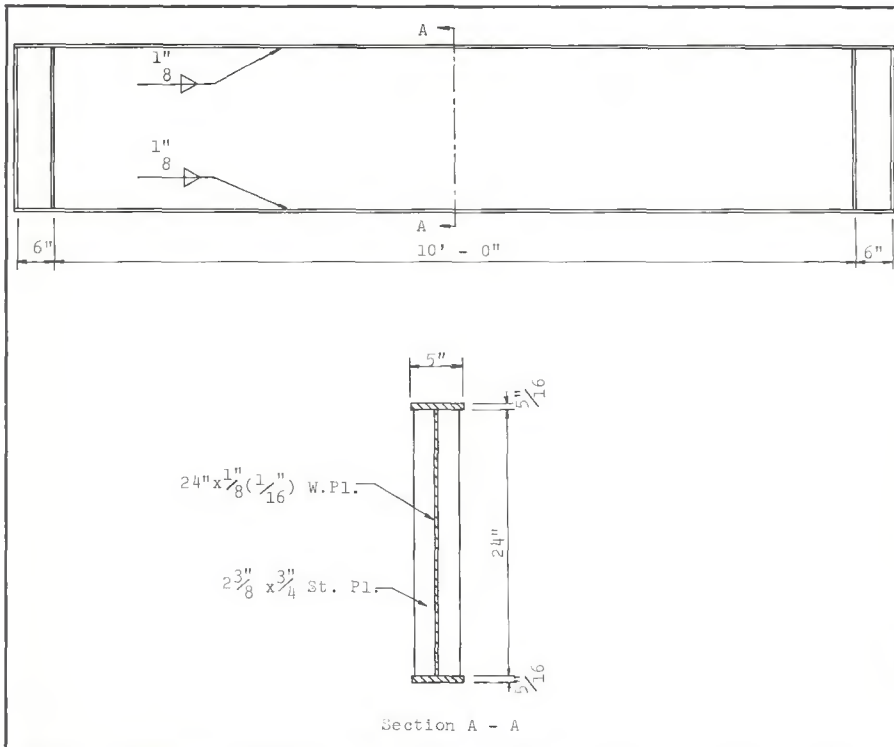


Fig. 1 — Elevations and vertical section of test girders

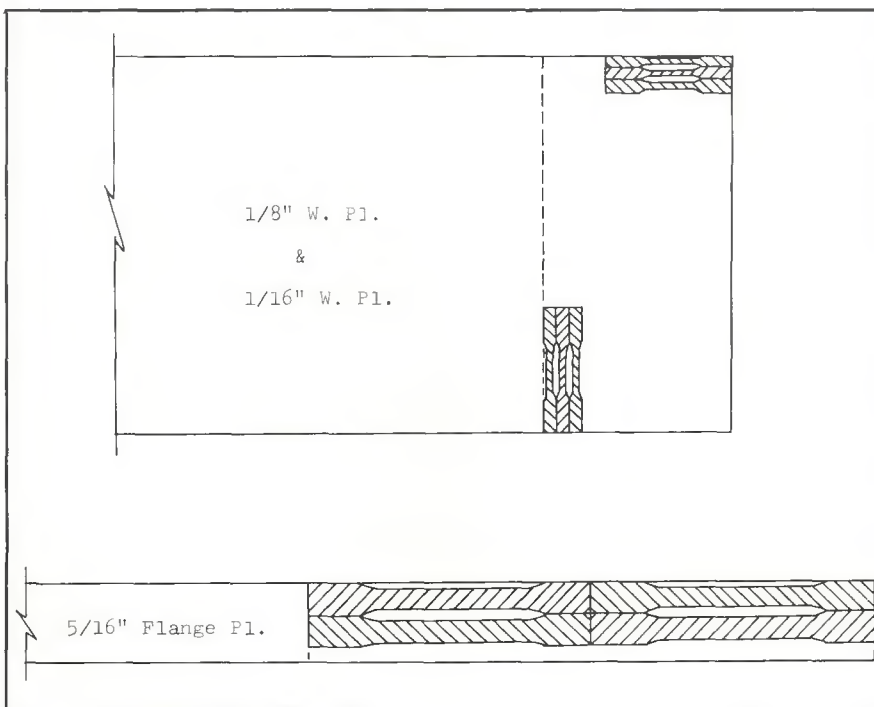


Fig. 2 — Location of tensile coupons

of bearing stiffeners at both ends. One of the girders with  $\frac{1}{8}$  in. web thickness was called 'Girder A' and the other with  $\frac{1}{16}$  in. web thickness was called 'Girder B.'

The dimensions of the components of girders A and B are provided on Table 1 and are shown graphically in Fig. 1. It is seen that the aspect ratio (the ratio of the panel length to the web depth),  $\alpha$ , is the same for both girders. However, the web slender-ness ratios (the ratio of the web depth to web thickness),  $\beta$ , are 192 and 384, respectively. The centroidal axis of the girder, in this case, is located at the mid-depth of the web because of symmetry about both horizontal and vertical axes of the cross-section. When a girder is subjected to a uniformly distributed load over the entire span, the central portion of the girder web is subjected to relatively high moment and low shear. However, the portions of the web near the supports are subjected to relatively high shear and low moment. It was expected that a pronounced web deformed shape under static loads could be measured by means of a set of dial gages. The testing procedure and the testing technique will be described in details in the following paragraphs.

**Material Properties**

The original intention in the design of the test specimen was to have homogeneous girders with the same value of the static yield stress of 36 ksi in all components. However, it is difficult for the steel fabricator to supply such specimens with uniform yield stress. Instead, the fabricator will supply the specimens with the guarantee that the minimum yield stress in all components will be 36 ksi. Under such circumstances, the yield stress of the girder components was an unknown factor to the investigators. Hence, the laboratory coupon tests of the component plates were performed.

The location of the coupon plates on the component plates of the test specimens are shown in Fig. 2. The figure shows that the coupon plates were cut from the end of the web and the flange plates. Two groups of coupons, each group consisting of three coupons, were cut from the web plates. One group of the coupons is in the horizontal direction of the web and the other is in the vertical direction of the web. The shape and dimensions of the tensile coupons are presented in Fig. 3. According to Reference 2, the gage length of the tensile coupons for the flange plates should be 8 in. and for the web plates should be 2 in.

The tensile coupon tests were per-

formed by using a Tinius-Olsen universal testing machine. The stress-strain relationship of each coupon was plotted by means of automatic recording devices attached to the testing machine. Results of the tensile coupon tests are tabulated in Table 2. The stress values shown in Table 2 represent the average value of the tensile coupons from each group of cutting.

A typical stress-strain diagram of the material used is shown in Fig. 3. This diagram shows three distinct portions of elastic, plastic, and strain-hardening ranges. The static yield stress was defined by the intersection of two straight lines. One of the lines is drawn parallel to the elastic portion of the stress-strain curve, the other is obtained by connecting the two (or more) kink points, which were obtained by stopping the testing machine during the testing process and then allowing the load to settle to a steady value (see Ref. 2).

The percentage elongation, the percentage reduction in the cross-sectional area, and the ultimate strength of the coupons are also tabulated in Table 2. The static yield stresses of all component plates are higher than the value of 36 ksi. The range is from 37.9 ksi (flange plate) to 43.8 ksi (1/8 in. web plate).

#### Instrumentation

**Vertical Deflections.** Locations for the reading of the vertical deflection of the girders are shown in Fig. 4. Ames dial gages with graduations of one thousandth and ten thousandths of an inch were used. The gages were placed in the same locations for the

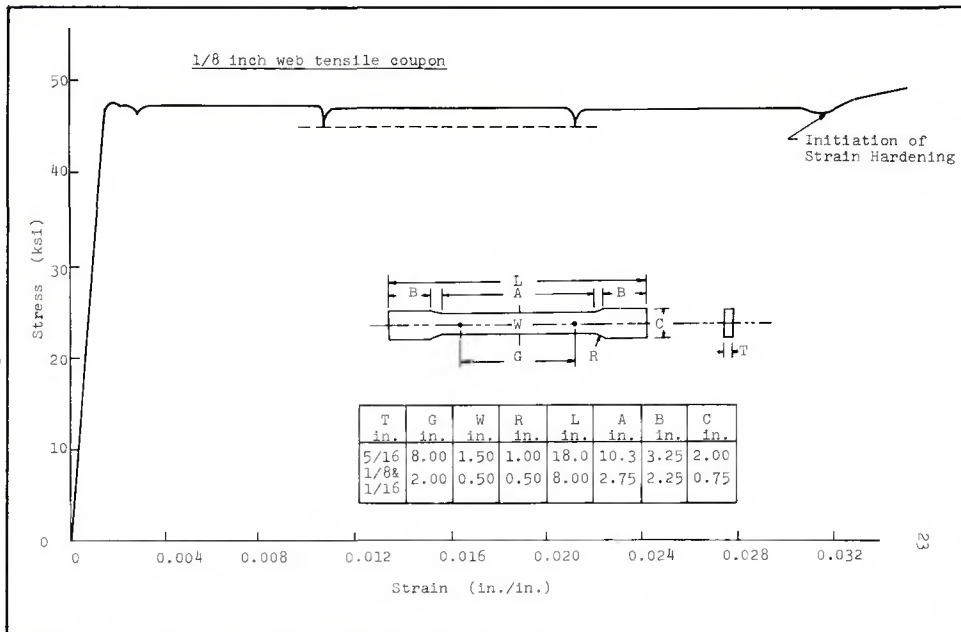


Fig. 3 — Stress-strain curve for tensile coupons

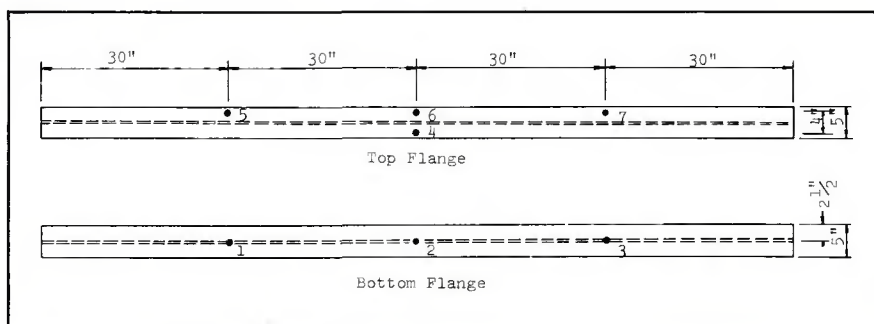


Fig. 4 — Location of dial gages

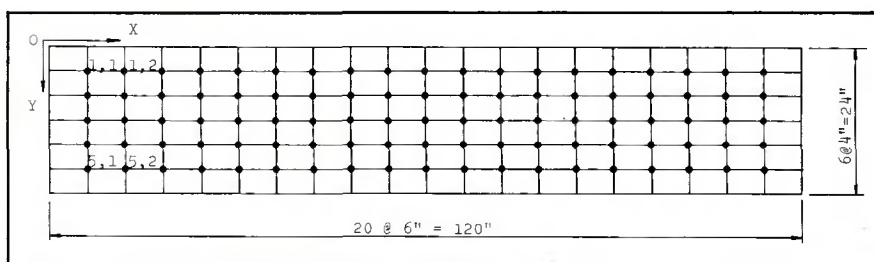


Fig. 5 — Location of web measurements

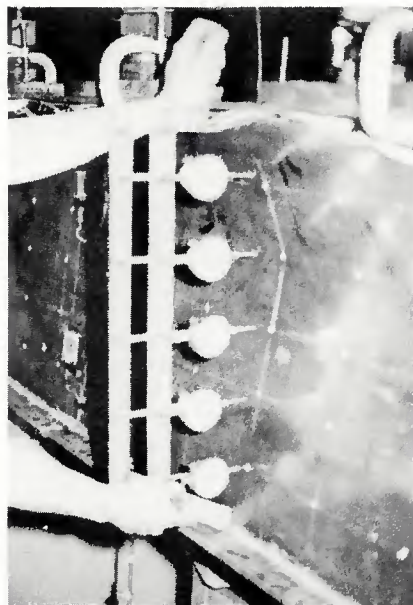


Fig. 6 — Web deflection measurements

Table 2 — Material Properties

Component	$\sigma_y$ , ksi	Tensile tests		
		$\sigma_u$ , ksi	Elong., %	Red. area, %
5/16 in. flange	37.9	60.6	31.5	43.2
1/8 in. web				
Horiz.	41.8	57.3	37.5	49.8
Vert.	43.8	59.4	34.5	52.1
1/16 in. web				
Horiz.	42.3	61.5	42.2	37.8
Vert.	42.0	65.5	39.1	32.6

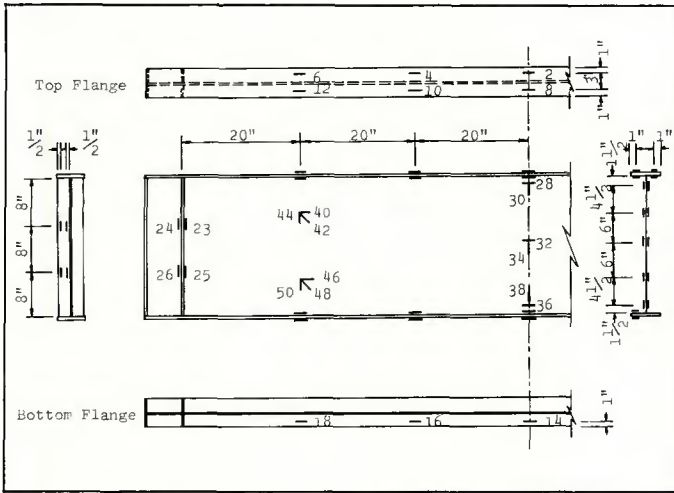


Fig. 7 — Strain gage location of girder A

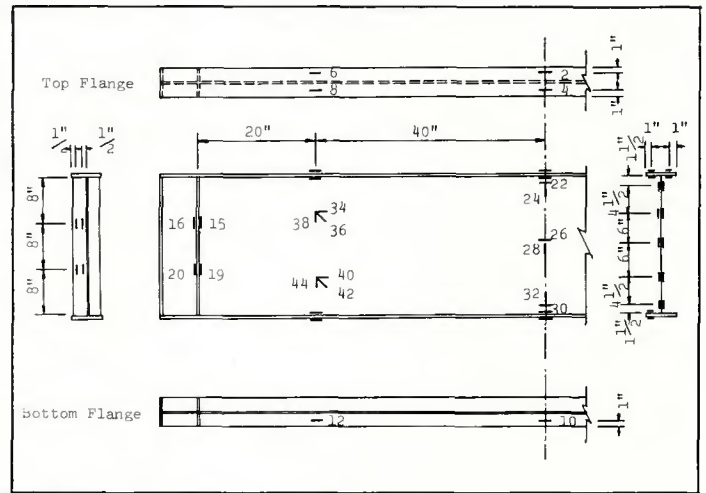


Fig. 8 — Strain gage location of girder B

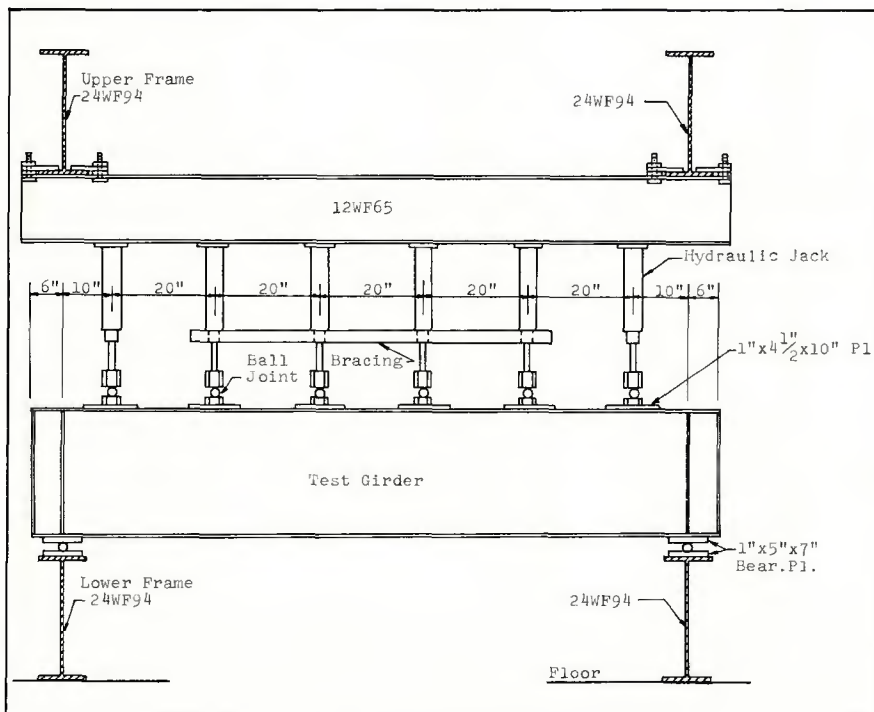


Fig. 9 — Front view of test setup

two girders. The numbers shown in the figure represent the designated number of the dial gages.

**Lateral Web Deflections.** The stations at which lateral deflection readings were taken are shown in Fig. 5. The x- and y-coordinate for each station are designated by the number of columns and the number of rows as shown in the figure. Five dial gages attached to the steel dial gage rib were used to measure the lateral deflections of the web under each loading increment. The locations of the dial gages in the y-direction were fixed through out the tests. Prior to each testing cycle, the dial gage rib was placed against a flat reference plane and thus a set of reference readings for each dial gage was obtained. The

application of the dial gage rib to obtain the web deflection readings is shown in Fig. 6. The lower arm of the dial gage rib is placed against the intersection of the web plate and the bottom flange. The upper arm of the rib is placed along the edge of the top flange. Under this arrangement, the web deflection readings are the relative values with respect to the flanges.

**Strain Measurements.** Three types of electrical resistance strain gages were used to measure the strains. The gages used were SR-4, A-1-S6 linear gages and SR-4, AR-1-S6 rosettes for girder A, and SR-4, FAP-25-12 linear gages and SR-4, AR-1-S6 rosettes for girder B. The gage factor for all gages is approximately 2.02.

Linear strain gages were placed at

the locations where the direction of the principal stresses were known. Rosettes were placed at the locations where the direction of the principal stresses were unknown. The locations of strain gages for girder A and B are shown in Figs. 7 and 8, respectively.

Strain measurements were read by means of a BLH strain indicator which was connected to a 10-channel BLH and a 20-channel Young switching box.

#### Test Setup

The loading system used in this testing program consisted of a set of six Energpac hydraulic jacks (Model No. 22-092) connected to a Riehle pumping unit. The hydraulic jacks have an effective piston area advance of 1.77 sq in. and an advance stroke of 10 in. The hydraulic pumping unit is equipped with two 'M' type gage indicators. One of the gage indicators has a range from 0 psi to 4,000 psi with a scale of 10 psi per division. The other indicator has a range from 0 psi to 10,000 psi with 20 psi per division.

The test girders were simply supported at both ends. The front view of the general test set-up is shown in Fig. 9. The loads were applied from a set of hydraulic jacks to the top flange of the girder through the spherical bearing joints. The compression flange of the girder was braced laterally at both ends and at the two one-third points of the flange by means of paired  $1\frac{1}{2} \times 1\frac{1}{2} \times \frac{1}{8}$  in. steel angles, shown in Figs. 10 and 11. Lateral bracing to the hydraulic jacks at the lower portion of the main shaft were also provided and are shown in Figs. 9, 14 and 15.

#### Testing Procedures and Results

##### Introduction

In this section the behavior of the girder during the course of testing will

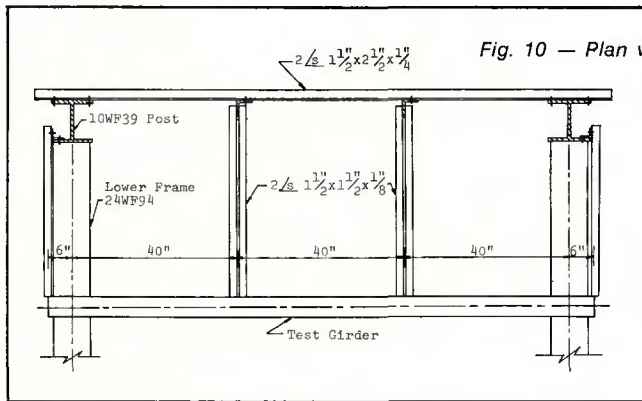


Fig. 10 — Plan view of test setup

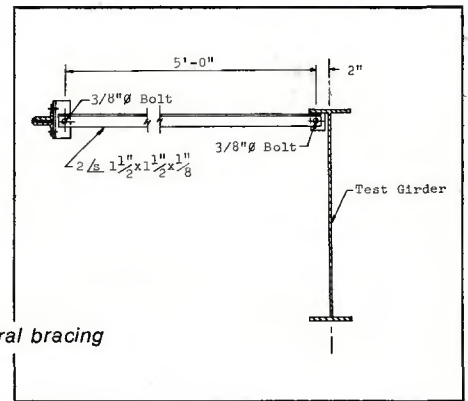


Fig. 11 — Lateral bracing

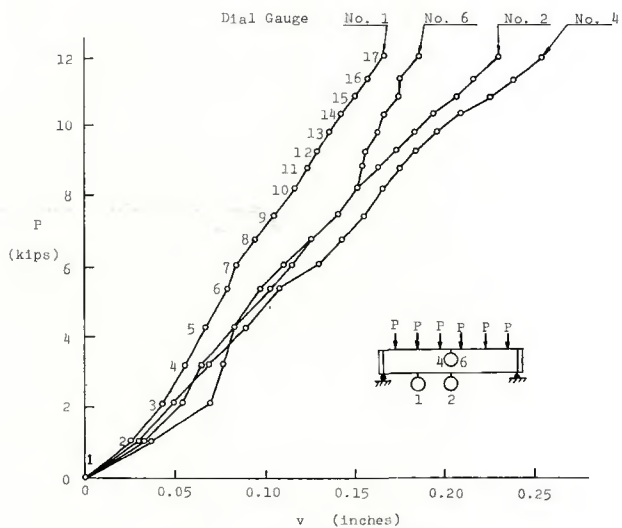
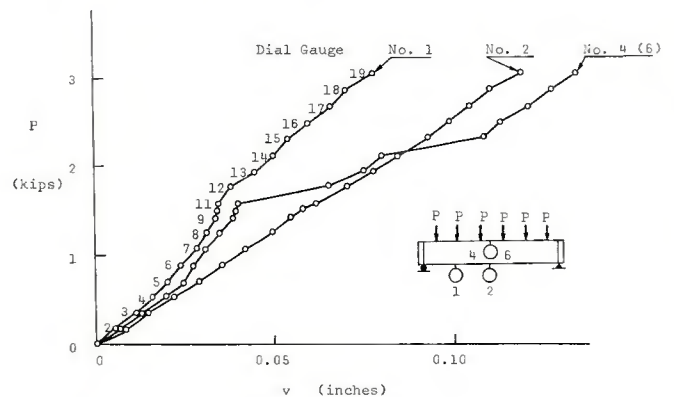


Fig. 12 — Load vs. vertical deflection of girder A

Fig. 13 — Load vs. vertical deflection of girder B



be described in detail. The results of the tests are expressed in terms of the applied jack load,  $P$  (single jack load), versus the following parameters: mid-span deflections of the tension flange and of the compression flange, the deflections of the tension flange at the one-third point of the span, the lateral deflections of the web plate, and the stress distributions over a vertical cross-section of the girder.

Prior to each testing cycle, a set of initial readings was taken for all measurements described previously. Then a certain increment of the load was gradually applied to the specimen. A set of readings for all measurements again was taken after the readings of the vertical deflection gages were stabilized. The ultimate load was considered reached when a continuous increase in the deflection was observed with essentially no increase in the applied load.

The coordinate system used for the following discussion is shown in the left upper portion of Fig. 5. The  $y$ -axis is located at the center line of the left bearing stiffeners with positive direc-

tion pointing downward. The  $x$ -axis is located along the web-top flange junction and the positive direction is to the right. The  $z$ -axis is in the di-

rection perpendicular to the plane of the web plate. The side of the specimen in the positive  $z$ -direction is called the 'inner side' while the opposite

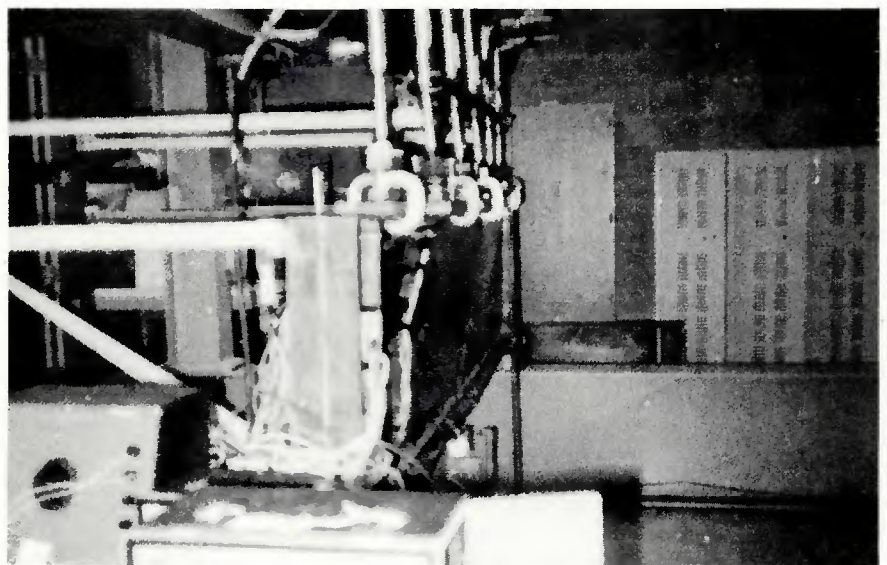


Fig. 14 — Girder A after failure load

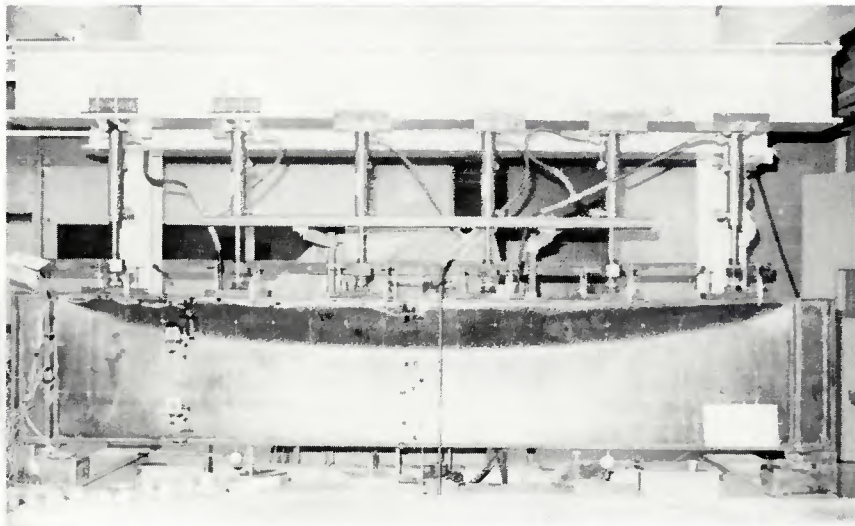


Fig. 15 — Girder B after failure load

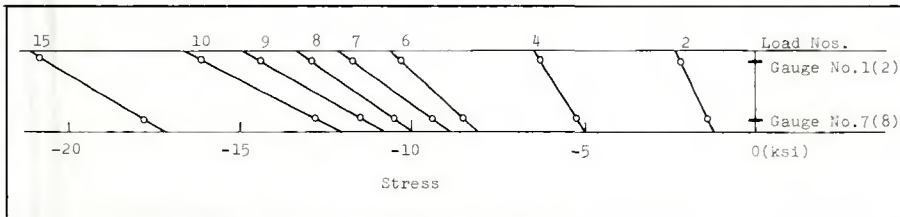


Fig. 16 — Stress distribution across top flange of girder A

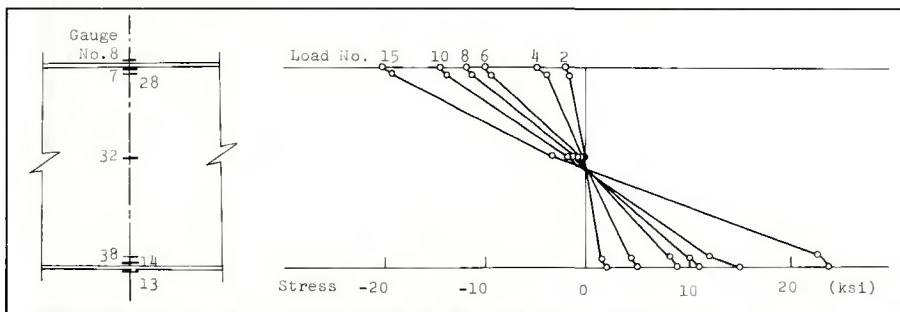


Fig. 17 — Stress distribution at mid-span of girder A

side is called the 'outer side.' The top flanges in the outer side of the girders were attached to the lateral bracing as shown in Figs. 10 and 14.

#### General Girder Behavior

The overall behavior of each test specimen is depicted in the load-deflection diagrams shown in Figs. 12 and 13. Dial gage No. 1, shown in the figures, is the measurement of the tension flange deflection at the one-third point of the span. Dial gage No. 2, No. 4 and No. 6 indicate the mid-span deflections of the tension flange and of the compression flange, respectively. In both Figs. 12 and 13, the numerical values shown along the performance curves of dial gage No. 1

are designated as the loading number in the course of testing.

**Girder A.** According to the above-mentioned measuring procedure, a set of initial readings for all measurements was taken prior to the application of the jack load to the specimen. Referring to the load No. 1 shown in Fig. 12, the jack load  $P$  was zero and the vertical deflection readings of the girder were also set to zero accordingly. Then the load was gradually increased to load No. 2 in the increment of 600 psi (1.06 kips per jack). The measuring process was repeated thereafter.

No significant lateral movement of the girder components was detected between load No. 1 ( $P=0$  kip) and load No. 9 ( $P=7.44$  kips).

Progressively developed bulge forms were observed in both end portions of the web plate after load No. 9, but there was still no significant indication of the lateral movement of the compression flange.

At load No. 17 ( $P=11.85$  kips), a pronounced bulge form of the web plate was observed. The readings in the gage indicator of the pumping unit and in the dial gages for the vertical deflections were still in steady state. However, force in the lateral bracings of the compression flange was detected. This was primarily due to the inward movement (in the direction of positive  $z$ -axis) of the compression flange.

An attempt to increase the jack load from load No. 17 to the next increment was not successful because the compression portion of the web plate deformed continuously and at the same time the compression flange started to rotate about the  $x$ -axis. The failure mode of girder A was a combination of the web plate buckling as well as the lateral buckling of the compression flange. Girder A after the failure load is shown in Fig. 14. It was noted that one of the lateral braces of the compression flange at the one-third point of the span was broken at the instance of failure, as shown in Fig. 14.

**Girder B.** The test setup and the testing procedure for girder B were similar to those for girder A. Because of a relatively high value of the web slenderness ratio of girder B ( $\beta=384$ ), a series of wave-shape wrinkles in the direction perpendicular to the longitudinal axis of the girder web was noticeable (see Fig. 23). This type of initial web imperfection was primarily due to uneven heating in the process of welding.

As shown in Fig. 13, no significant movement of the compression flange was observed between load No. 1 ( $P=0$  kip) and load No. 14 ( $P=2.13$  kips). No force on the lateral bracing was detected. However, the initial set of wrinkles in the web developed gradually into two bulge forms. It was interesting to note that the lateral deflections of the web plate in the two bulge forms were in the same direction.

As the successive load increments were applied to the girder, a more pronounced bulge form was observed. When the load No. 20 ( $P=3.22$  kips, not shown in the figure) was applied, the two bulge forms developed into a single one. As soon as the single bulge form was created, the girder reduced its load carrying capacity. The failure mode of girder B after failure is shown in Fig. 15. A well pronounced symmetrical buckling mode of the web plate about the vertical axis at the mid-span can be observed in this figure.

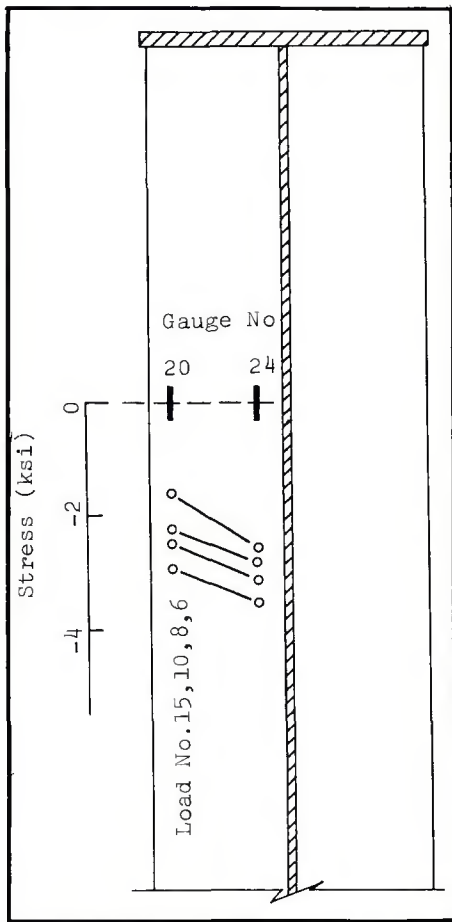


Fig. 18 — Stress distribution on the stiffener of girder A

### Stress Distributions

The strain gage readings were converted into stresses and shown graphically in Figs. 16, 17 and 18. The plot shows the stress distribution over the width of the compression flange of girder A is first presented in Fig. 16. It is noted that the stress in the outer

fiber of the compression flange is greater than that in the inner fiber. The stress variation over the width of the flange was caused by the inward movement of the flange during the test.

The stress in the x-direction at the mid-span section was plotted for girder A and is shown in Fig. 17. It is noted that the stresses in the web near the flange is less than the stress in the flange. The stress at point  $y = 1$  in. (strain gage No. 28), for example, is less than the stress at point  $y = 0$  in. (strain gage No. 7) as shown in Fig. 17.

The stresses on the bearing stiffeners for girder A were plotted in Fig. 18. A higher stress value is observed in the location closer to the web plate.

### Lateral Web Deflections

The lateral deflections of the web plate for girders A and B at sections  $x = 30, 60$  and  $90$  in. are plotted in Figs. 19 and 20, respectively. The jack load  $P$  versus web deflection relationships for girders A and B are also included in the figures. No significant web lateral deflection was observed when the applied jack load,  $P$ , was relatively low. The web, however, deflected rapidly when the load was in the vicinity of the ultimate load. It is interesting to note that the ultimate capacity of the unstiffened girder will be reached as soon as the web deflects rapidly in the lateral direction.

No sign of post-buckling tension field action was observed in either girders A or B. This seems to indicate that the girder collapses right after buckling of the web.

The contour maps for web lateral deflections are plotted, respectively, for girders A and B at zero load and at the failure load. Figure 21 shows that

the web plate of girder A was quite flat initially, and finally developed into a single bulge form at failure load (Fig. 22). The ridge of the bulge form is seen in a parabolic shape. A more pronounced lateral web deflection was observed for girders with thinner webs. Figures 23, 24 and 25 illustrate the deformed patterns of the web for girder B. It is noted that the scale of the maps and the interval of the contour lines are the same in all of the contour maps, so that a direct comparison of the lateral deformed shapes of the web plate can be made.

### Conclusions and Recommendations

The primary objective of the experimental investigation of the unstiffened thin web girders was to obtain information about the behavior of the girder web under a uniformly distributed load. The results of this investigation may be summarized as follows:

1. An unstiffened girder carries load like an ordinary beam before buckling of the web plate.
2. The girder collapses as soon as the web plate deflects rapidly in the lateral direction. No significant post-buckling tension field action was observed in this experiment.
3. The web plate of girder A, which has the web slenderness ratio of 192 and the compression flange area to web area ratio of about 0.5, behaves like a rectangular plate with clamped edges along the bearing stiffeners and the tension flange and simply supported along the compression flange.
4. The web plate of girder B, which has the web slenderness ratio of 384 and the compression flange area to web area ratio of about 1.0, behaves like a rectangular plate with four

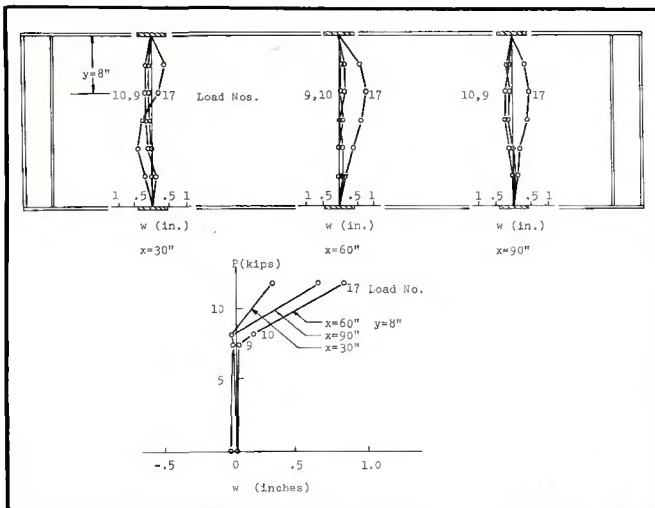


Fig. 19 — Web deflections for girder A

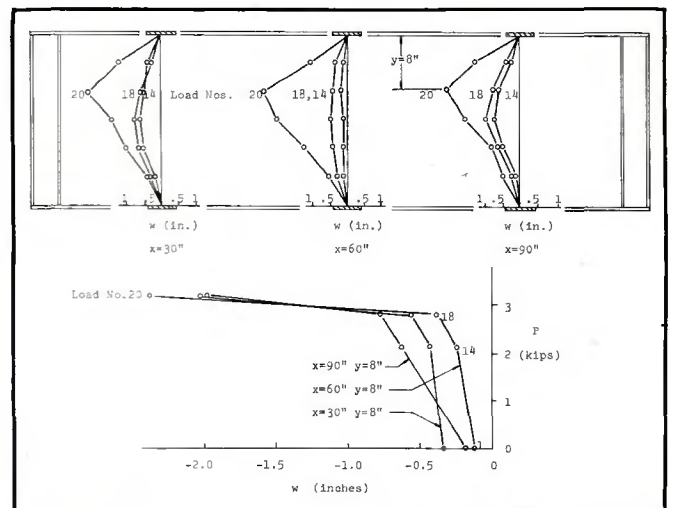


Fig. 20 — Web deflections for girder B

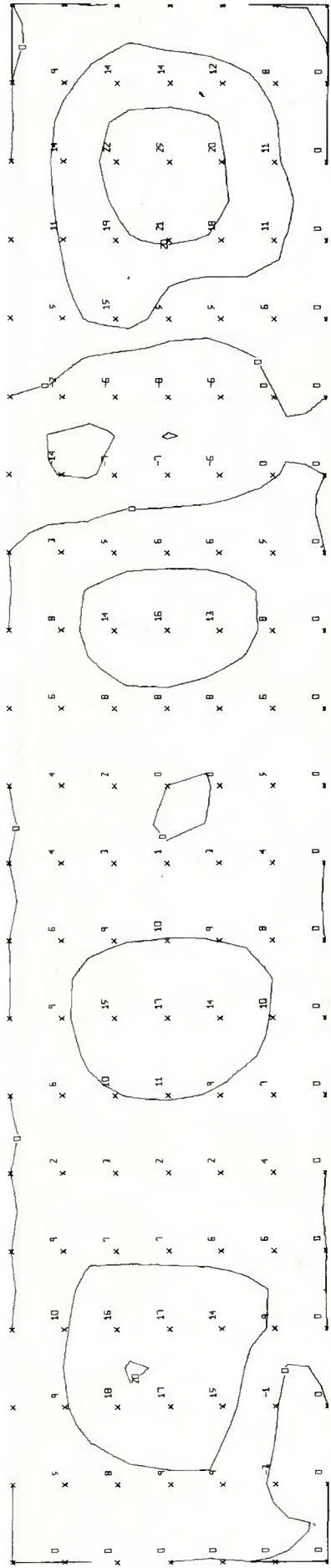


Fig. 21 — Web contour map of girder A at load  $P = 0$  kip

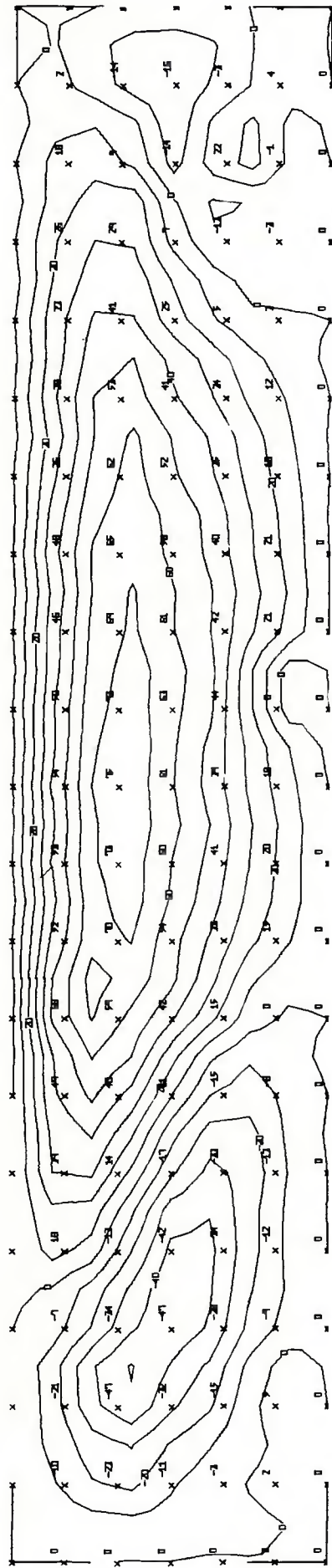


Fig. 22 — Web contour map of girder A at failure load

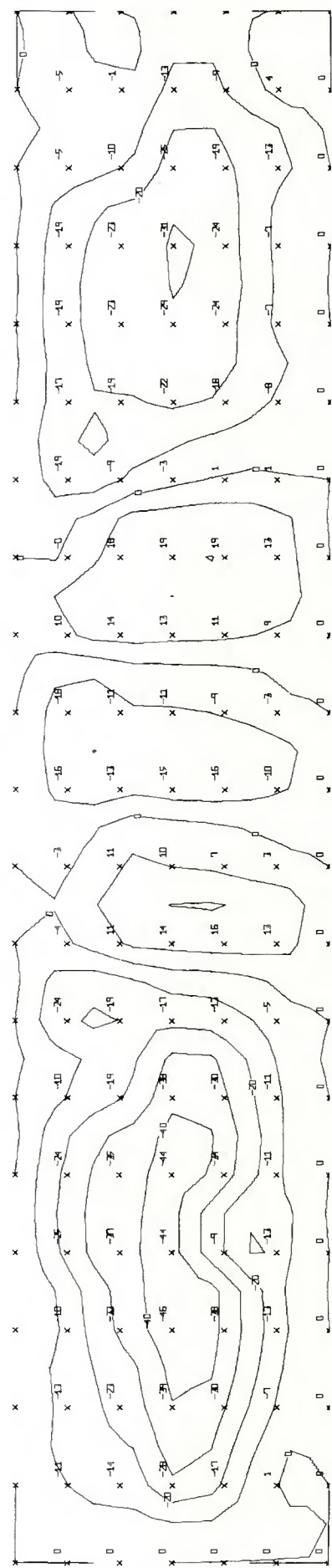


Fig. 23 — Web contour map of girder B at load  $P = 0$  kip

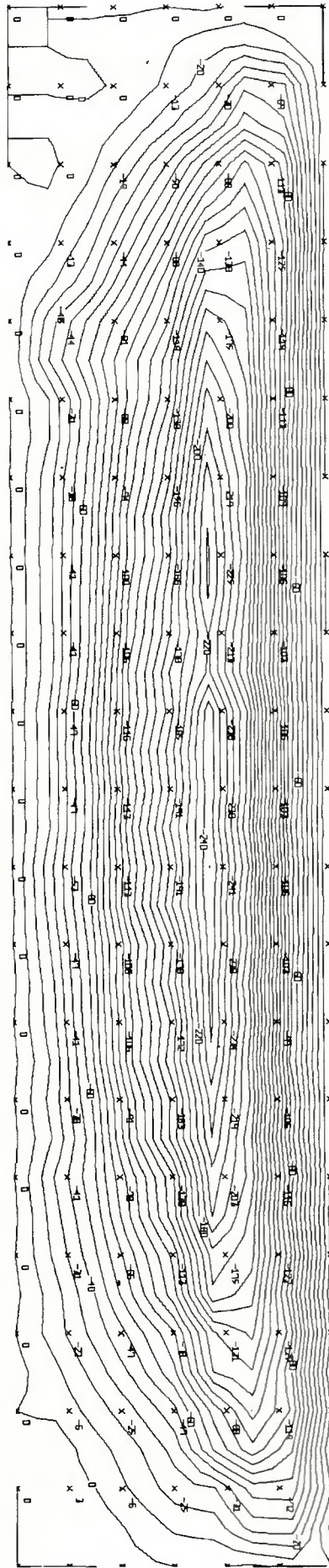
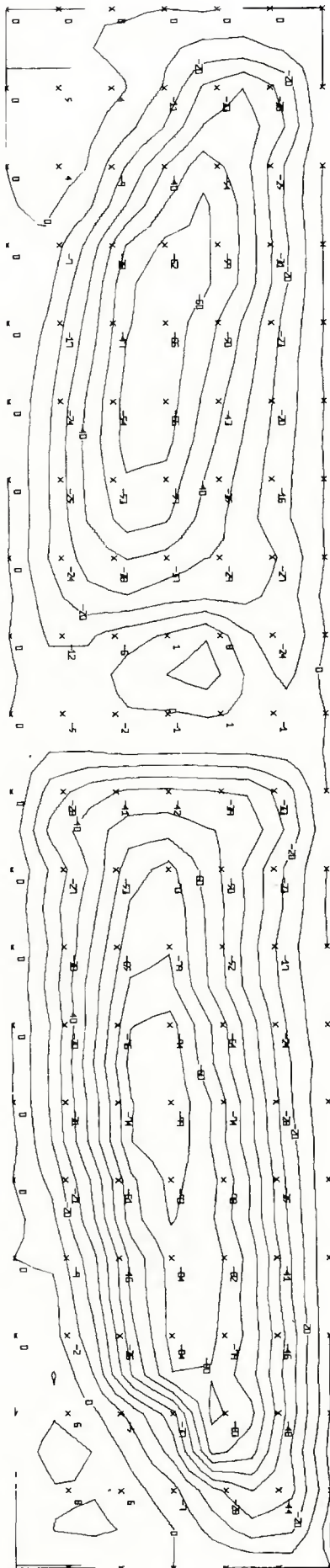


Fig. 24 (Left) — Web contour map of girder B at load  $P = 3.0$  kips (load No. 19)

Fig. 25 (Right) — Web contour map of girder B after failure

edges clamped.

Recommendations for further research in the area of unstiffened thin web girders may be drawn as follows:

1. Effect of web openings on the strength of unstiffened thin web girders.
2. Strength of composite unstiffened thin web girders, that is, a girder with the centroidal axis close to its compression flange.
3. Strength of thin web girders with a corrugated web.

#### References

1. American Institute of Steel Construction, *Specification for the Design, Fabrication, and Erection of Structural Steel for Buildings*, AISC, New York, 1970
2. American Society for Testing and Materials *ASTM Standards, Part 4*, 1970
3. Basler, K., Yen, B. T., Mueller, J. A., and Thurlimann, B., *Web Buckling Tests on Welded Plate Girders*, Bulletin No. 64, Welding Research Council, New York, September, 1960
4. Bergfelt, A., *Studies and Tests on Slender Plate Girders Without Intermediate Stiffeners*, Chalmers University of Technology, Sweden, March, 1971
5. Bossert, T. W., and Ostapenko, A., *Buckling Analysis of Plate Girder Webs*, Fritz Engineering Laboratory Report No. 319.2, Lehigh University, July, 1967
6. Chern, C., and Tungsi, P., *Strength of Unstiffened Thin Web Girders*, Department of Civil Engineering, North Dakota State University, June, 1972
7. Johnston, B. J. (Editor), *Guide to Design Criteria for Metal Compression Members*, Column Research Council, New York, 1966
8. Schueller, W., and Ostapenko, A., *Tests of Unsymmetrical Plate Girders — Main Test Series*, Fritz Engineering Laboratory Report No. 328.6, Lehigh University, September, 1968

#### Acknowledgements

This paper entitled "Experiments on Unstiffened Thin Web Girders" presents a part of the research project on unstiffened plate girders conducted in the Department of Civil Engineering, North Dakota State University, Fargo, North Dakota. Dr. James L. Jorgenson is the Chairman of the Department.

The project was sponsored by the Department of Civil Engineering, North Dakota State University.